

MedChemComm

Accepted Manuscript



This is an *Accepted Manuscript*, which has been through the Royal Society of Chemistry peer review process and has been accepted for publication.

Accepted Manuscripts are published online shortly after acceptance, before technical editing, formatting and proof reading. Using this free service, authors can make their results available to the community, in citable form, before we publish the edited article. We will replace this *Accepted Manuscript* with the edited and formatted *Advance Article* as soon as it is available.

You can find more information about *Accepted Manuscripts* in the [Information for Authors](#).

Please note that technical editing may introduce minor changes to the text and/or graphics, which may alter content. The journal's standard [Terms & Conditions](#) and the [Ethical guidelines](#) still apply. In no event shall the Royal Society of Chemistry be held responsible for any errors or omissions in this *Accepted Manuscript* or any consequences arising from the use of any information it contains.

Structure-Based Design, Synthesis by Click Chemistry and *in Vivo*

Activity of Highly Selective A₃ Adenosine Receptor Agonists

Dilip K. Tosh,[†] Silvia Paoletta,[†] Zhoumou Chen,[‡] Steven Crane,[†] John Lloyd,[†]

Zhan-Guo Gao,[†] Elizabeth T. Gizewski,[§] John A. Auchampach,[§]

Daniela Salvemini,[‡] and Kenneth A. Jacobson^{†*}

[†]Laboratory of Bioorganic Chemistry, National Institute of Diabetes and Digestive and Kidney Diseases, National Institutes of Health, Bethesda, MD 20892 USA.

[‡]Department of Pharmacological and Physiological Science, Saint Louis University School of Medicine, St. Louis, Missouri 63104 USA.

[§]Department of Pharmacology, Medical College of Wisconsin, 8701 Watertown Plank Road, Milwaukee, Wisconsin 53226 USA.

Corresponding author: Dr. K. A. Jacobson, Chief, Molecular Recognition Section, Bldg. 8A, Rm. B1A-19, NIH, NIDDK, LBC, Bethesda, MD 20892-0810 USA. *Tel:* 301-496-9024. *Fax:* 301-480-8422; *Email:* kennethj@niddk.nih.gov

ABBREVIATIONS: AR, adenosine receptor; cAMP, adenosine 3',5'-cyclic monophosphate; CCI, chronic constriction injury; CHO, Chinese hamster ovary; CNS, central nervous system; DIC, *N,N'*-diisopropylcarbodiimide; DMEM, Dulbecco's modified Eagle medium; DMF, *N,N*-dimethylformamide; EL, extracellular loop; GPCR, G protein-coupled receptor; HEPES, 2-[4-(2-hydroxyethyl)piperazin-1-yl]ethanesulfonic acid; HEK, human embryonic kidney; HPLC, high performance liquid chromatography; HRMS, high resolution mass spectroscopy; MW, molecular weight; NECA, 5'-N-ethylcarboxamidoadenosine; NMR, nuclear magnetic resonance; PBS, phosphate buffered saline; TSPO, translocator protein; PWT, Paw Withdrawal Threshold; RMS, root-mean-square; SAR, structure-activity relationship; TBAP, tetrabutylammonium dihydrogenphosphate; TEA, triethylamine; THF, tetrahydrofuran; TLC, thin layer chromatography; TM, transmembrane helix; tPSA, total polar surface area.

Abstract

2-Arylethynyl derivatives of (N)-methanocarba adenosine 5'-uronamides are selective A₃AR (adenosine receptor) agonists. Here we substitute a 1,2,3-triazol-1-yl linker in place of the rigid, linear ethynyl group to eliminate its potential metabolic liability. Docking of nucleosides containing possible short linker moieties at the adenine C2 position using a hybrid molecular model of the A₃AR (based on the A_{2A}AR agonist-bound structure) correctly predicted that a triazole would maintain the A₃AR selectivity, due to its ability to fit a narrow cleft in the receptor. The analogues with various N⁶ and C2-aryltriazolyl substitution were synthesized and characterized in binding (K_i at hA₃AR 0.3 – 12 nM) and *in vivo* to demonstrate efficacy in controlling chronic neuropathic pain (chronic constriction injury). Among N⁶-methyl derivatives, a terminal pyrimidin-2-yl group in **9** (MRS7116) increased duration of action (36% pain protection at 3 h) *in vivo*. N⁶-Ethyl 5-chlorothien-2-yl analogue **15** (MRS7126) preserved *in vivo* efficacy (85% protection at 1 h) with short duration. Larger N⁶ groups, e.g. **17** (MRS7138, >90% protection at 1 and 3 h), greatly enhanced *in vivo* activity. Thus, we have combined structure-based methods and phenotypic screening to identify nucleoside derivatives of having translational potential.

Keywords: G protein-coupled receptor; nucleoside; click chemistry; neuropathic pain; molecular modeling.

Introduction

Two nucleoside agonists of the A₃ adenosine receptor (A₃AR) are currently in clinical trials for the treatment of autoimmune inflammatory diseases (*N*⁶-(3-iodobenzyl)-5'-*N*-methylcarboxamidoadenosine, IB-MECA), including rheumatoid arthritis and plaque psoriasis, and hepatocellular carcinoma (2-chloro analogue, Cl-IB-MECA).^{1,2} An even broader range of conditions have been shown to be ameliorated by administration of A₃AR agonists in animal models, including osteoarthritis, neutropenia, and other inflammatory and infective conditions and chronic neuropathic pain.^{3,4} Chronic neuropathic pain can result from injury or diseases such as cancer and diabetes or from pharmaceutical administration, and its treatment represents an unmet medical need. Thus, the design, synthesis and pharmacological characterization of novel drug-like A₃AR agonists of high affinity, selectivity and *in vivo* efficacy are well justified.

The selective A₃AR agonists that have advanced to clinical trials are adenine-9-riboside derivatives.^{1,2} As an extension of the structure activity relationship (SAR) of AR agonists, we have introduced nucleoside derivatives containing in place of ribose a bicyclo[3.1.0]hexane (methanocarba) ring system, which display increased affinity and/or selectivity for the A₃AR compared to other AR subtypes.⁵ The rigid ribose ring substitute maintains a receptor-preferred conformation and thus decreases an entropic energy barrier for receptor binding. Prototypical nucleosides containing a methanocarba ring system in a North (N) envelope conformation are typically >100-fold more potent at the

A₃AR than the corresponding isomers in the South (S) conformation.⁶ A combination of A₃AR-favoring modifications provided MRS5698 **1** and MRS5980 **2** (Chart 1A) as highly potent agonists with favorable protective properties in the sciatic nerve chronic constriction injury (CCI) model of neuropathic pain in mice.⁷⁻⁹ These rigidified nucleosides contain a C2-arylethynyl group,¹⁰ which is thought to be responsible for the high A₃AR selectivity, based on the greater structural plasticity of the A₃AR compared to the A_{2A}AR, which is more constrained by disulfide bridges in the extracellular loops (ELs). In particular, we have proposed an outward movement of transmembrane helix 2 (TM2) in the A₃AR in order to accommodate the C2-arylethynyl group and still to maintain conserved H-bonding interactions of the hydroxyls of the ribose-like moiety with the N⁶ and N7 of the adenine moiety.^{7,11}

However, the presence of an arylethynyl group might be an indication of potential liver toxicity due to its electrophilicity and possible reactivity with glutathione.¹² Therefore, we explored alternative structures that would still maintain the proper geometry of the distal aryl group with respect to the adenosine core structure. A number of alternative C2 substituents were considered and compared by docking to an A₃AR model: benzyl **3b**, phenylethyl **3c**, phenylcyclopropyl **3d**, phenyl-*trans*-ethenyl **3e**, and phenyl-triazolyl **3f** (Chart 1A, Ar = C₆H₅). A 1,2,3-triazol-1-yl group was predicted to best maintain a similar geometry compared to the potent and selective C2-arylethynyl derivatives.

This work has multiple goals: 1) to identify a general class of compounds that are highly selective agonists of the A₃AR but do not contain an arylethynyl group, based initially on

a comparison of hypothetical structures using molecular modeling; 2) to determine the *in vivo* efficacy and duration of action in a mouse model of neuropathic pain in order to select preferred candidates for further development.

Results and discussion

We used molecular modeling to predict the effect of logical C2 modifications **3b-f** (R = CH₃, Ar = C₆H₅) on human (h) A₃AR recognition. Because the rigid, elongated C2 substituent of the series of general formula **3a** is key to the >3000-fold A₃AR selectivity vs. the A_{2A}AR, a substitution for the ethynyl group would need to maintain a similar extended conformation when bound to the receptor. The receptor model used for docking was our recently published hybrid homology model of the A₃AR.^{7,11} The agonist-bound hA_{2A}AR X-ray structure¹³ was used as a template for all of the TMs, except for the upper part of TM2.¹¹ Figure 1 compares the effects of these substitutions when the nucleosides are docked in the hybrid model, and Table 1 summarizes the features of the different proposed linkers (substitutes for C≡C of **3a**). Docking simulations showed that all the derivatives bearing the proposed alternative C2 substituents were able to fit the binding site of the A₃AR hybrid model in an orientation analogous to the one observed for the original arylethynyl derivatives. Such a binding pose has been well validated in previous studies^{7,11} and shows all the interactions key for agonist binding at ARs.¹³ In particular, the pseudo-sugar moiety forms H-bonds with Thr94 (3.36), Ser271 (7.42) and His272 (7.43) (numbers in parenthesis follow the Ballesteros-Weinstein numbering system),¹⁴ the adenine core forms two H-bonds with Asn250 (6.55) and a π - π stacking with Phe168

(EL2), the N^6 substituent interacts with hydrophobic residues on EL2 such as Val169 and the C2 group is directed towards TM2 (Figure 1A).

Thus, to select the best linker to be used in the new series of derivatives, we analyzed the various alternatives in a detailed manner. The rigid, elongated C2 substituent is a key feature for high A_3AR selectivity, because of the greater structural plasticity of the A_3AR compared to the $A_{2A}AR$ as previously proposed,⁷ therefore we predicted higher selectivity at the A_3AR for those derivatives bearing rigid and elongated linkers, such as **3d-f**. These substitutions might approximate the docked position of the terminal aryl group of known selective agonist series **3a** (Figure 1A).

The terminal phenyl ring need not be coplanar with the adenine ring, but a substantial bending within the C2 substituent would not be favored. Compounds **3b** and **3c**, even though predicted to bind the A_3AR , would probably interact also with the $A_{2A}AR$ because of flexibility in the position of the terminal phenyl ring, possibly resulting in reduced selectivity. Moreover, the C2 linker is accommodated in a narrow region between Phe168 (EL2) and Ile268 (7.39) (~ 4 Å, Figure 1B). Therefore, we predicted a higher affinity at the A_3AR for those derivatives bearing a planar linker, such as **3a**, **3e** and **3f**, compared to those with wider and out-of-plane linkers, such as **3b-d**. In light of these considerations, compounds **3e** and **3f** would be the best alternatives to preserve the high affinity and selectivity of the arylolethynyl group. However, because of the potential chemical and photochemical reactivity of a styryl group, we decided not to synthesize derivatives of compound **3e** but to focus on triazolyl derivatives. In fact, as highlighted in Table 1,

triazole series **3f** seemed to be the best alternative to alkynyl series **3a**, because of its stability, its rigid, planar and elongated C2 group (Figure S1, Supporting information) and its synthetic feasibility. The terminal phenyl rings of **3a** and **3f** are largely overlapping when docked to the A₃AR. However, **3f** is slightly more elongated than **3a** (by 0.8 Å), and it was shown previously that rigid C2 substituents more extended than phenylethynyl are tolerated at the A₃AR.⁷

Nucleoside derivatives **5** - **20** (Table 2) were synthesized by the route shown in Scheme 1. The previous series of aryethynyl derivatives was prepared by a Sonogashira reaction¹⁵ of a substituted arylacetylene with a C2-iodo derivative of a (N)-methanocarba adenosine. Here we access the triazole derivatives via a click reaction, [3+2] cycloaddition of a congeneric set of 2-azidoadenosines (**30** – **34**) and arylacetylenes,¹⁶ which link adenine and C2-terminal aryl moieties (Scheme 1). The azide group is introduced on adenine via reaction of sodium azide with the corresponding 2-iodo intermediates (**25** – **29**), which were prepared as described from L-ribose.¹⁷ The product 2-(1,2,3-triazol-1-yl) nucleosides that were subsequently tested in binding assays were demonstrated using HPLC to be of high purity (>95%). Click chemistry of (N)-methanocarba adenosines was used previously to prepare various high affinity A₃AR ligands.¹⁸

Radioligand binding assays were performed at three subtypes of hARs that are relevant for this chemical series and at the mouse (m) A₃AR, which were stably expressed in mammalian cells, as previously reported (Table 2).^{7,8} An unusual ferrocene-ethynyl

derivative **4** was included as a reference compound due to its prolonged *in vivo* activity and for comparison to its triazole analogue **20**.⁸ Representative binding curves are shown in Supporting Information. As predicted using the 3D model of the hA₃AR, the affinity and selectivity of the *N*⁶-methyl and *N*⁶-ethyl [1,2,3]triazolyl derivatives (**5** – **15**, **19**, **20**) were extremely high. All of the derivatives (**5** – **34**) displayed K_i values in the range of 0.3 – 12 nM at the A₃AR, but larger *N*⁶ groups, i.e. **16** – **18**, reduced selectivity by increasing A₁AR affinity. The 2-iodo and 2-azido intermediates (**25** – **34**) were even less selective in comparison to the A₁AR and A_{2A}AR. Thus, the triazolyl spacer constitutes a suitable replacement for the ethynyl group with respect to the receptor binding profile. Also, a triazole group like an alkyne is uncharged at physiological pH. A set of A₃AR-selective triazolyl derivatives in the 9-ribose series of adenosine agonists was reported previously,¹⁹ and this (N)-methanocarba series extends the finding of high A₃AR affinity in the present set of analogues, and with comparable or greater selectivity. There is a correlation ($r^2 = 0.66$) between the A₃AR binding affinity of twelve *N*⁶-methyl C2-triazolyl derivatives reported here and the corresponding ethynyl derivatives (Figure 2). This is consistent with the hypothesis that the terminal aryl ring occupies a similar position in the two series when bound to the A₃AR, as shown in Figure 2. Binding of selected compounds at the mA₃AR indicated that a C2-triazolyl-5-chlorothien-2-yl group in compounds **15** – **17** maintained a relatively high affinity in the range of 7 – 14 nM with various *N*⁶ groups. Curiously, the C2-triazolyl-pyrimidin-2-yl derivative **9** was much less potent than other analogues at the mA₃AR. The ligand efficiency²⁰ with respect to A₃AR affinity was favorable: **1**, 0.23; **2**, 0.33; **9**, 0.27; **15**, 0.31; **17**, 0.24.

After confirming the A₃AR-selectivity, the A₃AR agonists were screened *in vivo* in the mouse CCI model.²¹ The protection by A₃AR agonists against chronic neuropathic pain occurs at both central and peripheral sites of action.¹¹ The methods used were as reported,^{7,8} and the agonist was given by oral gavage (3 µmol/kg) on day 7 after sciatic nerve ligation, i.e. the time when peak pain develops. The paw withdrawal threshold (PWT) was measured up to 5 h after drug administration. The maximal efficacy *in vivo* and the duration of action were indicated (Table 3). Each compound reached its peak protection against chronic neuropathic pain by 1 h after administration. In the earlier alkynyl series⁸ peak protection was achieved between 0.5 and 2 h after administration and maintained up to 3 h (as with 5-chlorothieryl derivative **2**, which suppressed neuropathic pain to the degree of 83% protection at 3 h). By comparison, compound **1** at the same dose displayed only 24% protection after 3 h.⁸ Here, at 1 h after drug treatment the mechanoallodynia was a nearly completely reversed by some triazole derivatives, i.e. pyrimidin-2-yl **9**, *N*-methylpyrazolyl **11**, 5-chlorothieryl-2-yl **15** and 5-bromothieryl-2-yl **19** analogues and compounds **16** – **18**. For *N*⁶-methyl analogues, the majority of the pain protection by the triazolyl derivatives waned by the 3 h time point (Figures 3A,B). In analogues containing the same terminal 5-chlorothiophene group found in very efficacious and long-acting agonist **2**, an *N*⁶-ethyl group in **15** compared to the *N*⁶-methyl homologue **14** produced a higher maximal protection at 1 h, i.e. 85% vs. 67%, respectively. A 2-pyrimidyl group in **9** favored duration of action *in vivo*, with 36% of the protection remaining at 3 h, which would not have been predicted by its relatively weak mA₃AR affinity. Larger *N*⁶ groups, e.g. 3-chlorobenzyl in **17** (>90% protection at 1 and 3 h), combined with a terminal chlorothieryl group greatly enhanced *in vivo* activity

(Figure 3C). At a lower dose (1 $\mu\text{mol/kg}$), **17** produced the same duration of protection but the maximal effect reached a plateau at $\sim 70\%$ (Figure S2, Supporting Information). *N*⁶-Cyclobutyl **16** and *N*⁶-(2-phenylethyl) **18** derivatives were also prolonged in activity.

There is some consistency of the *in vivo* results between triazole and ethynyl series. For example, a ferrocene group present in ethynyl derivative **4** and triazole **20** was associated with high efficacy *in vivo*, although *in vitro* stability tests indicated that **4** was subject to rapid degradation ($t_{1/2}$ in human liver microsomes and pH 1.6 simulated stomach acid of 3.66 and 46.5 min, respectively).⁸ Therefore, we used mass spectrometry (Figures S3-S6, Supporting information) to identify the immediate, transient product of acidic decomposition of **4** upon exposure to aqueous HCl at pH 1.6. The result indicated a rapid loss of Fe-cyclopentadiene as detected within 5 min by mass, leaving a cyclopentadiene moiety remaining on the nucleoside (**39**, Chart 1B); however, **39** was highly unstable and unable to be isolated. The corresponding cyclopentadiene **40** in the triazole series was not detected upon incubation at pH 1.6 of **20**, which was stable. Therefore, the substitution of the 2-alkyne spacer with triazole increased the chemical stability of the ferrocene derivative. This might result from greater delocalization of the ferrocene electron density in the direction of adenine moiety in the extended triazole-linked aromatic system, rendering the ferrocene moiety less readily protonated.

Off-target activities of several triazole derivatives (**12**, **14**) were also determined in a broad receptor binding screen (Supporting Information).²² The only interactions at $\text{IC}_{50} < 10 \mu\text{M}$ were with H_2 histamine (**12**, 50% inhibition at 10 μM) and sigma2 receptors (**12**,

50%; **14**, 62%) and the peripheral benzodiazepine receptor (TSPO, **14**, 54%). These few interactions reinforced the A₃AR selectivity of these representative compounds.

Conclusions

Derivatives of selective A₃AR agonists containing a triazole linker in place of an ethynyl group, a preferred substitution as predicted using molecular modeling, were prepared and shown to parallel the ethynyl series in receptor affinity and selectivity. Docking of possible linker moieties at the C2 position, using a molecular model of the A₃AR, correctly predicted that the receptor affinity and selectivity would be maintained due to common structural features that favored selective binding at the A₃AR. A planar C2-triazole linker fit well in a narrow cleft when docked in the receptor binding site. The effects of N⁶ substitution were also probed. All of these analogues contain a (N)-methanocarpa ring system to optimize A₃AR affinity, which improves the selectivity in comparison to the ribose series.⁵

The analogues were characterized in binding and *in vivo* assays to demonstrate efficacy in controlling chronic neuropathic pain in agreement with A₃AR selectivity. An N⁶-ethyl group in **15** preserved *in vivo* activity compared to N⁶-methyl and binding selectivity, while larger groups reduced A₃AR selectivity. In comparison to the activities of the corresponding 2-arylethynyl derivatives, the duration of action of many analogues tended to be shorter.⁸ Nevertheless, among N⁶-methyl derivatives a terminal pyrimidin-2-yl group in **9** extended the duration of action compared to other aryl groups. A highly prolonged and full efficacy in reversing mechanoallodynia was achieved in a few

derivatives, i.e. **16** – **18** that contained larger N^6 substitution. The most enhanced *in vivo* efficacy and duration was seen with N^6 -(3-chlorobenzyl derivative **17** (nearly full protection up to 4 h).

The use of X-ray structures of closely related GPCRs in homology modeling, docking and screening has facilitated understanding ligand recognition and drug discovery for the A_3AR and for other receptors.²³ Here, the effects of potential structural changes were probed computationally to select preferred structures to synthesize. The use of a phenotypic assay, i.e. the CCI model, provides much information on efficacy, duration of action and indirectly oral bioavailability. Thus, this study has progressed from the stage of structure-based design to a comparison of molecules having the desired pharmacological properties in *in vitro* and *in vivo* preclinical experiments. We have combined efficient methods to narrow the group of nucleoside derivatives of potential translational interest.

Acknowledgements

This research was supported in part by the Intramural Research Program of the NIH, National Institute of Diabetes and Digestive and Kidney Diseases, and NIH R01 HL077707). We thank Noel Whittaker (NIDDK) for mass spectral determinations. We thank Dr. Bryan L. Roth (Univ. North Carolina at Chapel Hill) and National Institute of Mental Health's Psychoactive Drug Screening Program (Contract # HHSN-271-2008-00025-C) for screening data.

Supporting information

Supplementary data (chemical synthesis, characterization data, calculations and results of *in vivo* experiments, modeling procedures and off-target screening) associated with this article can be found in the online version, at doi:.

Notes and references

- ¹ Silverman, M. H., Strand, V., Markovits, D., Nahir, M., Reitblat, T., Molad, Y., Rosner, I., Rozenbaum, M., Mader, R., Adawi, M., Caspi, D., Tishler, M., Langevitz, P., Rubinow, A., Friedman, J., Green, L., Tanay, A., Ochaion, A., Cohen, S., Kerns, W. D., Cohn, I., Fishman-Furman, S., Farbstein, M., Yehuda, S. B., Fishman, P. *J. Rheumatol.* 2008, **35**, 41.
- ² Bar-Yehuda S., Stemmer S. M., Madi L., Castel D., Ochaion A., Cohen S., Barer F., Zabutti A., Perez-Liz G., Del Valle, L., Fishman, P. *Int. J. Oncol.* 2008, **33**, 287.
- ³ Borea, P. A., Varani, K., Vincenzi, F., Baraldi, P.G., Tabrizi, M. A., Merighi, S., Gessi, S. *Pharmacol. Rev.* 2015, **67**, 74.
- ⁴ Chen, Z., Janes, K., Chen, C., Doyle, T., Tosh, D. K., Jacobson, K. A., Salvemini, D. *FASEB J.* 2012, **26**, 1855.
- ⁵ Tosh, D. K., Jacobson, K. A. *Med. Chem. Comm.* 2013, **4**, 619.
- ⁶ Jacobson, K. A., Ji, X. D., Li, A. H., Melman, N., Siddiqui, M. A., Shin, K. J., Marquez, V. E., Ravi, R. G. *J. Med. Chem.* 2000, **43**, 2196.
- ⁷ Tosh, D. K., Deflorian, F., Phan, K., Gao, Z. G., Wan, T. C., Gizewski, E., Auchampach, J. A., Jacobson, K. A. *J. Med. Chem.* 2012, **55**, 4847.
- ⁸ Tosh, D. K., Finley, A., Paoletta, S., Moss, S. M., Gao, Z. G., Gizewski, E., Auchampach, J., Salvemini, D., Jacobson, K. A. *J. Med. Chem.* 2014, **57**, 9901.
- ⁹ Little, J. W., Ford, A., Symons-Liguori A. M., Chen Z., Janes, K., Doyle, T., Xie, J., Luongo, L., Tosh, D. K., Maione, S., Bannister, K., Dickenson, A., Vanderah, T. W., Porreca, F., Jacobson, K. A., Salvemini, D. *Brain* 2015, **138**, 28.
- ¹⁰ Dal Ben, D., Buccioni, M., Lambertucci, C., Marucci, G., Volpini, R., Cristalli, G. *Curr. Med. Chem.* 2011, **18**, 1444.
- ¹¹ Paoletta, S., Tosh, D. K., Finley, A., Gizewski, E., Moss, S. M., Gao, Z. G., Auchampach, J. A., Salvemini, D., Jacobson, K. A. *J. Med. Chem.* 2013, **56**, 5949.
- ¹² Edwards, P. J., Sturino, C. *Curr. Med. Chem.* 2011, **18**, 3116.
- ¹³ Xu, F., Wu, H., Katritch, V., Han, G. W., Jacobson, K. A., Gao, Z. G., Cherezov, V., Stevens, R. *Science* 2011, **332**, 322.
- ¹⁴ Ballesteros, J. A., Weinstein, H. *Methods Neurosci.* 1995, **25**, 366.
- ¹⁵ Chinchilla, R., Nájera, C. *Chem. Rev.* 2007, **107**, 87.
- ¹⁶ Kolb, H. C., Finn, M.G., Sharpless, K. B. *Angew. Chem. Int. Ed.* 2001, **40**, 2004.
- ¹⁷ Joshi, B. V., Melman, A., Mackman, R. L., Jacobson, K. A. *Nucleos. Nucleot. Nucleic Acids* 2008, **27**, 279.
- ¹⁸ Tosh, D. K., Chinn, M., Yoo, L. S., Kang, D. W., Luecke, H., Gao, Z. G., Jacobson, K. A. *Bioorg. Med. Chem.* 2010, **18**, 508.
- ¹⁹ Cosyn, L., Palaniappan, K. K., Kim, S. K., Duong, H.T., Gao, Z. G., Jacobson K. A., Van Calenbergh, S. *J. Med. Chem.* 2006, **49**, 7373.
- ²⁰ Hopkins, A. L., Groom, C. R., Alex, A. *Drug Discov. Today* 2004, **9**, 430.
- ²¹ Bennett, G. J., Xie, Y. K. *Pain* 1988, **33**, 87.
- ²² Paoletta, S., Tosh, D. K., Salvemini, D., Jacobson, K. A. *PLoS ONE* 2014, **9**, e97858.
- ²³ Mason, J. S., Bortolato, A., Weiss, D. R., Deflorian, F., Tehan, B., Marshall, F. H. *In Silico Pharmacology* 2013, **1**, 23, doi:10.1186/2193-9616-1-23.
- ²⁴ Cheng, Y. C., Prusoff, W. H. *Biochem. Pharmacol.* 1973, **22**, 3099.

- ²⁵ Melman, A., Gao, Z. G., Kumar, D., Wan, T. C., Gizewski, E., Auchampach, J. A., Jacobson, K. A. *Bioorg. Med. Chem. Lett.* 2008, **18**, 2813.

Figure and Scheme Legends

Chart 1. A. Structures of recently reported highly selective A₃AR agonists (**1**, **2**) and the structural options considered in the present study (**3**). R is a small alkyl, cycloalkyl or substituted arylalkyl group; Ar refers to substituted phenyl or heterocyclic groups or ferrocene (See compound **4**, Table 2). **B.** Hypothetical transient breakdown products **39** and **40** from acid treatment of the ferrocene derivatives **4** and **20**, respectively. Only **39** was detected by mass upon acidification of **4**; compound **20** was stable at pH 1.6.

Scheme 1. Synthesis of A₃AR agonists containing triazolyl spacers between the C2 position of adenine and a terminal aryl group. For the structures of **5** - **20** see Table 2.

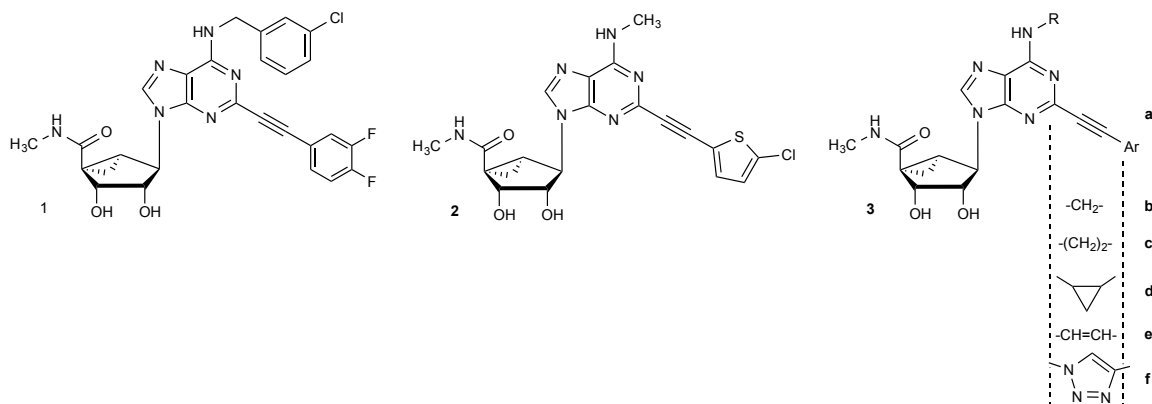
Figure 1. Superposition of the docking poses of trial compounds **3a** – **f** (R = CH₃, Ar = Ph) in the hA₃AR hybrid homology model. A. Side view of the receptor (shown in cyan ribbon). Ligands are shown in sticks with different carbon colors (**3a**, dark green; **3b**, orange; **3c**, pink; **3d**, yellow; **3e**, magenta; **3f**, light green). Side chains of residues important for ligand recognition are shown in sticks (grey carbons), and H-bonding interactions are indicated by red dashed lines. Non-polar hydrogen atoms are not displayed. The view of TM7 is partially omitted. B. Top view of the receptor showing the surface of the binding site residues in cyan. Ligands are shown in sticks with different carbon colors (color scheme as in panel A). The distance between Phe168 (EL2) and Ile268 (7.39) is highlighted.

Figure 2. Correlation of the binding affinities at the hA₃AR of parallel series of triazolyl (Y-axis) and ethynyl (X-axis) derivatives.⁸ The values shown include those determined for triazolyl compounds **5** – **14**, **19**, and **20**.

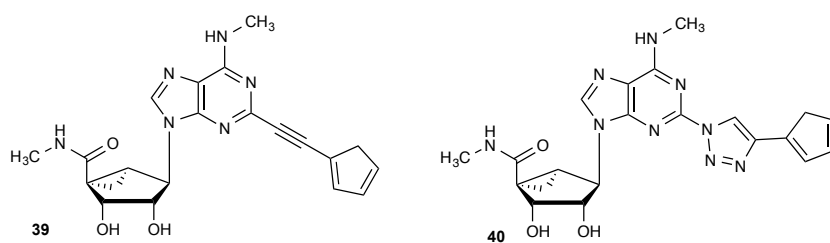
Figure 3. Protection against hind paw mechanoallodynia in mice resulting from CCI of the sciatic nerve. Triazolyl derivatives were administered at a single dose (p.o.) of 3 µmol/kg at the point of peak pain (7 days post surgery; representative curves of 2-4 determinations). A. Derivatives **5**, **6** and **8** – **10**, in which the terminal aryl group is a phenyl, substituted phenyl or six-membered heterocycle. B. Derivatives **7**, **11**, **13**, **19** and **20**, in which the terminal aryl group is a 3,4-difluorophenyl or five-membered heterocycle. C. Derivatives **16** – **18**, with large N⁶ substitution and in which the terminal aryl group is 5-chlorothien-2-yl. Data are mean ± SEM of n=2 or 4 and analyzed by two-tailed, two-way ANOVA with Bonferroni comparisons to D0 or D7/BL. *P<0.05 vs. D0 and †P<0.05 vs. D7/BL.

Chart 1.

A



B



Scheme 1.

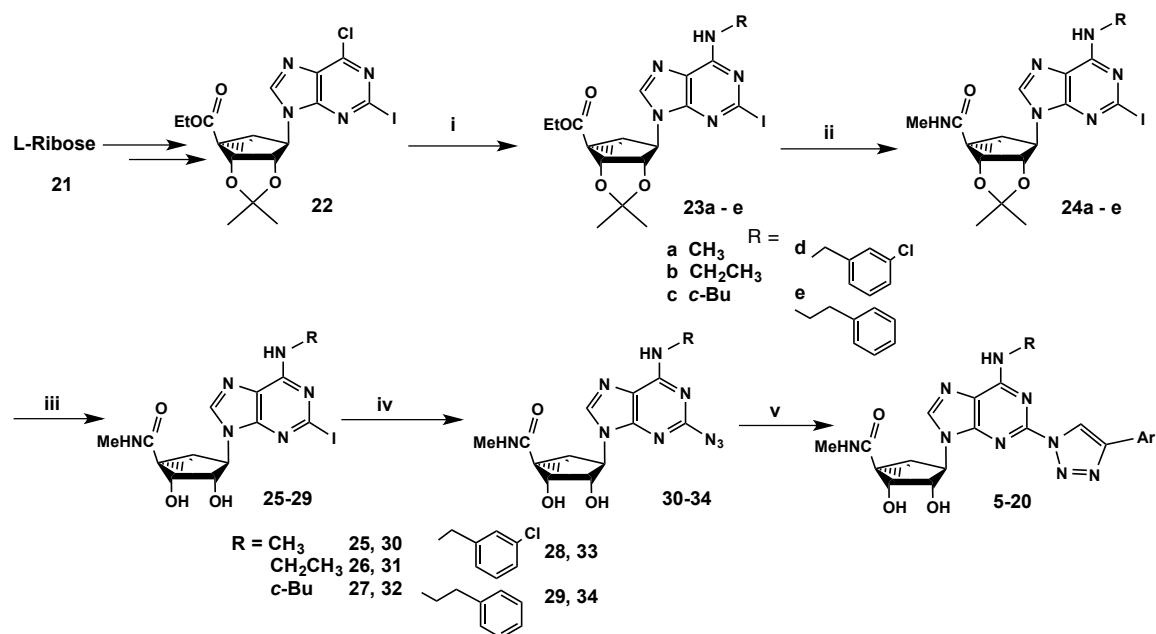


Figure 1.

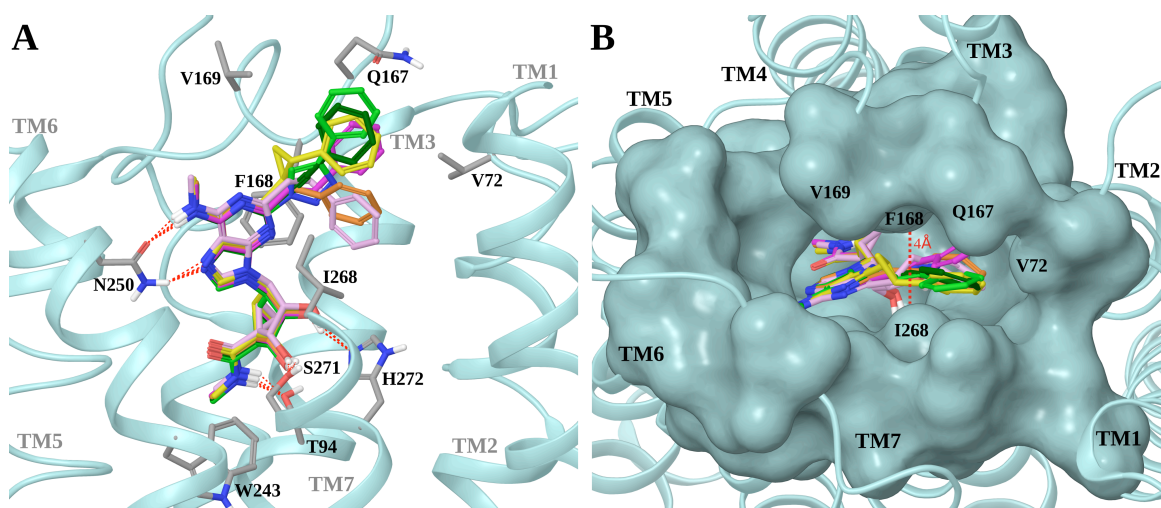


Figure 2.

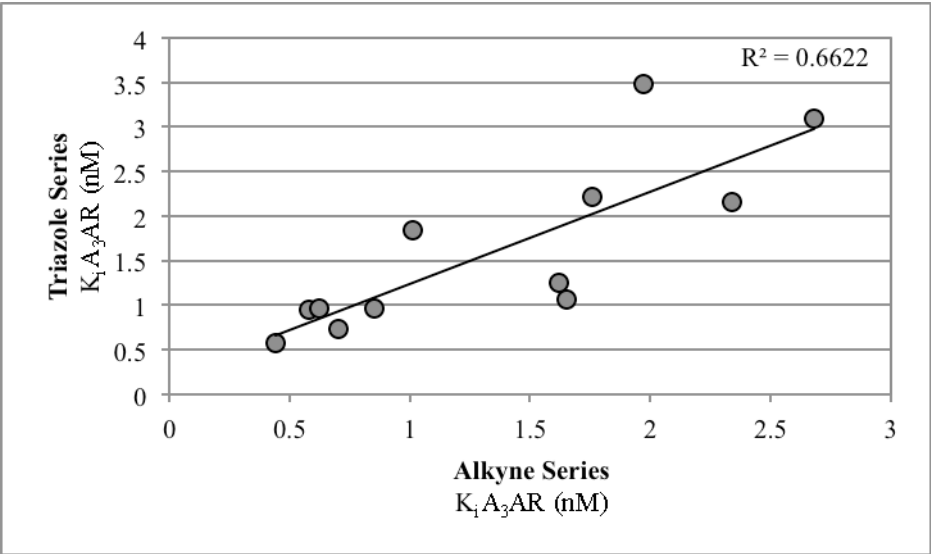


Figure 3.

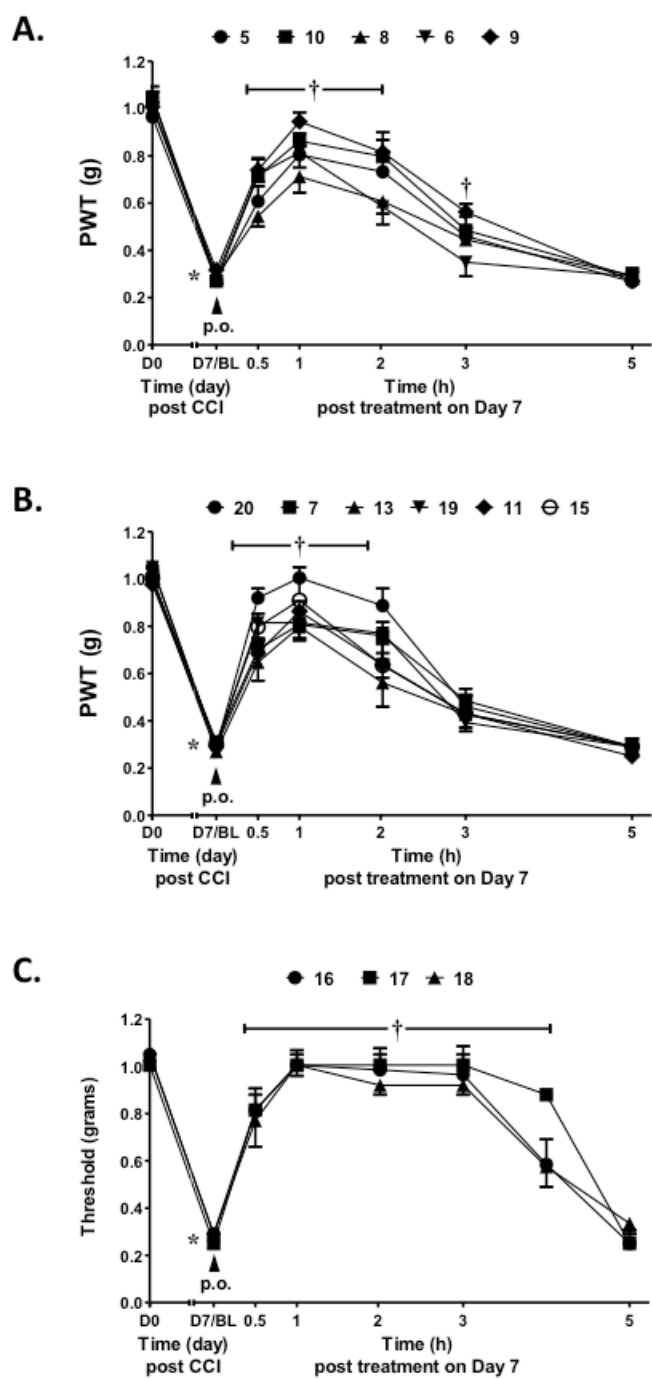


Table 1. Comparison of the features of C2 modifications **3a-f** (Chart 1A, Ar = C₆H₅). A check mark indicates favorable (planarity and rigidity, with respect to the binding cleft in the C2-extended adenine region of the A₃AR as in Figure 1) or unfavorable criteria (reactivity) as applied to each linker. All of the maximum lengths shown are within the range of the proposed outward displacement of TM2 in the hybrid A₃AR model.

	Linker	Linker Features			
		Planarity ^a	Rigidity ^b	Max Length ^c	Potential Reactivity ^d
a	C≡C	✓	✓	8.00	✓
b	CH ₂			6.37	
c	(CH ₂) ₂			5.84	
d	cyclopropyl		✓	7.61	
e	CH=CH	✓	✓	7.70	✓
f	triazole	✓	✓	8.80	

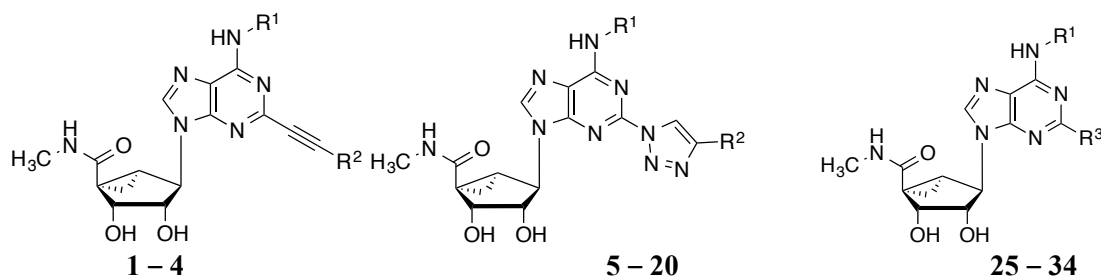
^a Ability to fit in a narrow space. This refers to the planarity of the linker only not of the overall C2 substituent.

^b Inability to bend.

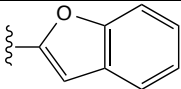
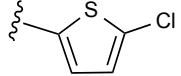
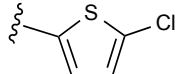
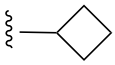
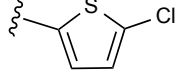
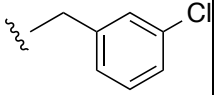
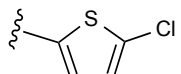
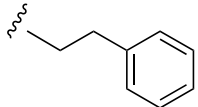
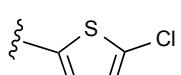
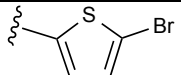
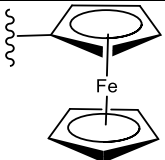
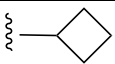
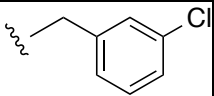
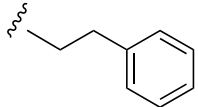

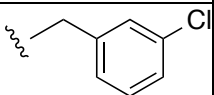
^c Distance measured between the C2 of the adenine core and the most distal hydrogen of the phenyl ring.

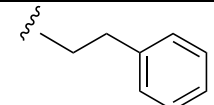
^d Potential toxicity and/or reactivity with nucleophiles *in vivo*.

Table 2. Structures and binding affinities^a of AR agonists, including reference compounds **1-4**, triazole derivatives **5-20** and their synthetic intermediates **25-34**.



Compd.	R ¹	R ² or R ³	A ₁ AR % inhibition or K _i (nM) ^a	A _{2A} AR % inhibition ^c	A ₃ AR % inhibition or K _i (nM) ^a
1^{b,d}			6 ± 4%	41 ± 10%	3.49±1.84, 3.08±0.23 (m)
2^{b,d}	CH ₃		6 ± 1%,	24 ± 13%,	0.70 ± 0.11, 36.1±4.7 (m)
4^{b,d}	CH ₃		25 ± 2%	47 ± 2%	2.68 ± 0.44
5^d	CH ₃		18 ± 4%	35 ± 8%	0.96 ± 0.07
6	CH ₃		20 ± 5%	31 ± 6%	0.95 ± 0.50
7	CH ₃		9 ± 4%	39 ± 4%	1.06 ± 0.10
8	CH ₃		29 ± 7%	26 ± 2%	1.84 ± 0.38
9	CH ₃		14 ± 7%	27 ± 3%	3.48 ± 0.97, 334 ± 49 (m)
10	CH ₃		25 ± 10%	8 ± 3%	2.21 ± 0.34
11	CH ₃		2 ± 2%	1 ± 1%	2.16 ± 0.32
12	CH ₃		43 ± 2%	51 ± 1%	0.96 ± 0.09

13	CH ₃		$12 \pm 7\%$	$40 \pm 6\%$	1.25 ± 0.27
14	CH ₃		$27 \pm 8\%$	$34 \pm 5\%$	0.73 ± 0.10
15 ^d	C ₂ H ₅		$15 \pm 11\%$	$32 \pm 5\%$	1.22 ± 0.26 , 9.64 ± 0.84 (m)
16			77%	ND	7.05 ± 5.81 , 14.2 ± 0.2 (m)
17			65%	ND	9.02 ± 5.78 , 6.53 ± 0.58 (m)
18			58%	ND	6.66 ± 2.07
19	CH ₃		$33 \pm 7\%$	$7 \pm 6\%$	0.58 ± 0.17
20	CH ₃		$23 \pm 3\%$	$54 \pm 2\%$	3.09 ± 0.21
25 ^b	CH ₃	I	ND	ND	1.91 ± 0.85
26	CH ₂ CH ₃	I	1910 ± 300	$11 \pm 7\%$	1.22 ± 0.21
27		I	93%	>10,000	1.53 ± 0.45
28 ^b		I	2200 ^e	>10,000	3.6
29		I	68%	42%	0.91 ± 0.14
30	CH ₃	N ₃	$77 \pm 1\%$	$1 \pm 1\%$	0.54 ± 0.10
31	CH ₂ CH ₃	N ₃	707 ± 152	$11 \pm 6\%$	0.69 ± 0.08
32		N ₃	100%	46%	0.85 ± 0.10
33		N ₃	ND	2770 ^e	1.08 ± 0.75

34		N ₃	93%	1110 ^e	0.85 ± 0.10
-----------	---	----------------	-----	-------------------	-------------

^a Binding in membranes prepared from CHO or HEK293 (A_{2A} only) cells stably expressing one of three hAR subtypes, unless noted. The binding affinity for hA₁, A_{2A} and A₃ARs was expressed as K_i values (n = 3–4, unless noted), measured using agonist radioligands [³H]N⁶-R-phenylisopropyladenosine **35**, [³H]2-[p-(2-carboxyethyl)phenylethylamino]-5'-N-ethylcarboxamido-adenosine **36**, or [¹²⁵I]N⁶-(4-amino-3-iodobenzyl)adenosine-5'-N-methyl-uronamide **37**, respectively. Additional values designated (m) are for mouse ARs. A percent in italics refers to inhibition of binding at 10 μM. Nonspecific binding was determined using **38** (10 μM). Values are expressed as the mean ± SEM. K_i values were calculated as reported.²⁴

^b Data from Tosh et al.^{7,8} and Melman et al.²⁵

^c Percent of inhibition at 10 μM.

^d **1**, MRS5698; **2**, MRS5980; **4**, MRS5979; **5**, MRS7110; **15**, MRS7126; **17**, MRS7138.

^e n = 1.

ND – not determined.

Table 3. Activity of orally administered A₃AR agonists (3 μmol/kg) in CCI model of neuropathic pain (mechanoallodynia) in mice and physicochemical parameters.

Compound	Max. effect	Effect at 3h	n	MW	cLogP ^b	tPSA
	E _{max} (%±SEM) ^a	(%±SEM)		(D)		(Å ²)
1	100 ± 0.0	23.7 ± 10.8	4	565	4.15	122
2	93.3 ± 6.7	82.8 ± 11.2	4	459	2.17	122
4	94.3 ± 5.7	78.1 ± 3.5	4	526	1.42	122
5	77.4±4.5	27.5±4.1	4	461	1.58	150
6	69.1±8.6	7.9±7.9	2	496	2.04	150
7	75.2±12.8	27.0±7.4	4	497	1.79	150
8	60.9±11.9	21.1±3.3	4	462	0.29	162
9	92.7±9.8	36.2±6.8	4	463	-0.67	175
10	76.6±0.9	26.6±6.3	4	463	-0.67	175
11	82.5±5.9	19.1±5.9	4	465	-0.31	165
12	65.3±8.2	21.1±7.0	2	451	0.96	159
13	74.0±10.7	22.3±8.3	4	502	2.34	159
14	66.8±19.4	8.4±7.2	2	502	2.19	150
15	84.9±14.0	17.9±12.6	4	515	2.72	150
16	90.7±6.0	85.2±9.0 4	4	542	3.10	150
17	94.7±3.1	91.0±4.5 4	4	612	4.35	150
18	94.1±5.9	82.9±5.3 2	2	592	4.29	150
19	69.1±8.6	13.5±2.3	2	546	2.34	150

20	94.1±5.9	22.4±6.6	2	569	1.22	165
-----------	----------	----------	---	-----	------	-----

^a Percent represents reversal of reduction in PWT of the ipsilateral hind paw. The time of peak for compounds **5** – **20** is 1 h. Data for **1**, **2** and **4** are from Tosh et al.⁸ No mechano-allodynia or A₃AR agonist effect on PWT was observed on the contralateral side.

^b calculated using ChemBioDraw, v. 14.0.